Available online at www.sciencedirect.com

SCIENCE DIRECT®

Inorganica Chimica Acta 357 (2004) 1523–1537

ELSEVIER

Inorganica Chimica Acta

www.elsevier.com/locate/ica

Synthesis and spectroscopic characterization (IR, ^{1}H and ^{31}P NMR, electrospray ionization mass) of mono-, di-, tetra- and poly-meric complexes of silver(I) with diphosphine ligands: X-ray crystal structures of $AgNO_2$:($Ph_2PCH_2PPh_2$) (1:1)$_2$, $AgNO_2$:($Ph_2P(CH_2)_3PPh_2$) (1:1)$_2$, $AgNO_2$:($Ph_2PCH{=}CHPPh_2$) (2:1)$_2$ and $AgNO_2$: {p-tolyl)$_2$P($C_{10}H_6$)$_2$P(p-tolyl)$_2$} (1:1) [☆]

Effendy [a,b], John V. Hanna [c], Fabio Marchetti [d], Domenico Martini [d], Claudio Pettinari [d,*], Riccardo Pettinari [d], Brian W. Skelton [b], Allan H. White [b]

[a] *Jurusan Kimia, FMIPA Universitas Negeri Malang, Jalan Surabaya 6, Malang 65145, Indonesia*
[b] *Department of Chemistry, The University of Western Australia, Crawley, WA 6009, Australia*
[c] *ANSTO NMR Facility, Materials Division, Private Mail Bag 1, Menai, NSW 2234, Australia*
[d] *Dipartimento di Scienze Chimiche, Università degli Studi di Camerino, via S. Agostino 1, 62032 Camerino MC, Italy*

Received 3 November 2003; accepted 8 November 2003

Abstract

Adducts of diphosphine ligands $R_2P(R')_nPR_2$ (dppm: R = Ph, R′ = CH_2, n = 1; dppe: R = Ph, R′ = CH_2, n = 2; dppp: R = Ph, R′ = CH_2, n = 3; dppb: R = Ph, R′ = CH_2, n = 4; dppf: R = Ph, R′ = ferrocenyl, n = 1; dppet: R = Ph, R′ = CH=CH, n = 1; dcpm: R = cy, R′ = CH_2, n = 1; S-Binap: R = Ph, R′ = (S)-(+)-1,1-binaphthyl, n = 1, n = 2; (R-Tol-Binap: R = p-tolyl; R′ = (R)-(+)-1,1-binaphthyl, n = 1; (S,S-Diop: R = Ph, R′ = (4S,5S-(+)-O-isopropylidene-2-3-dihydroxybutane, n = 1) with silver(I) nitrite have been synthesized and characterized both in solution (^{1}H, ^{31}P NMR, ESI MS) and in the solid state (IR, single crystal X-ray structure analysis, ^{31}P NMR). The topologies of the structures in the solid state were found to depend on the nature of the diphosphine and in some cases also on the stoichiometric ratio $AgNO_2$:$R_2P(R')_nPR_2$. The adducts $AgNO_2$:dppm (1:1)$_2$ and $AgNO_2$:dppp (1:1)$_2$ are dimers, the role of dppm and dppp being to bridge two silver centers with each nitrite O,O'-chelating. The adduct $AgNO_2$:dppet (2:1)$_2$ is tetranuclear, derivative of the chair form, the bidentate ligands bridging central and peripheral silver centers, the nitrite being coordinated through both oxygens, the first unidentate, the second bridging bidentate. R-Tol-Binap forms a mononuclear 1:1 adduct, with the nitrite an O,O'-chelate.

Keywords: Silver; ^{31}P NMR CPMAS; X-ray crystal structure; Diphosphine

1. Introduction

The versatile diphosphine ligands are particularly appropriate for the synthesis of low-valent metal complexes. Bis(diphenylphosphino)methane (dppm) and 1,2-bis(diphenylphosphino)ethane (dppe) are widely used in inorganic chemistry, bis(diphenylphosphino)methane affording binuclear metal complexes in the μ-dppm form, while dppe affords both chelating and bridging complexes. dppm Complexes containing the $M_2(dppm)_2$ structural unit have been intensively investigated [1–3]. Although a key feature of the chemistry of this class of complexes is the relatively stable and quasi-planar M_2P_4 framework where two metal atoms are connected by a pair of bridging dppm ligands, it is well known that a variety of structural possibilities can occur when low-valent metals are bonded to a bidentate phosphine and a labile ligand such as nitrate or carboxylate [4,5].

[☆] Supplementary data associated with this article can be found, in the online version, at doi: 10.1016/j.ica.2003.11.010.

[*] Corresponding author. Tel.: +39-0737-402234; fax: +39-0737-637345. *E-mail address:* claudio.pettinari@unicam.it (C. Pettinari).

0020-1693/$ - see front matter © 2003 Elsevier B.V. All rights reserved.
doi:10.1016/j.ica.2003.11.010

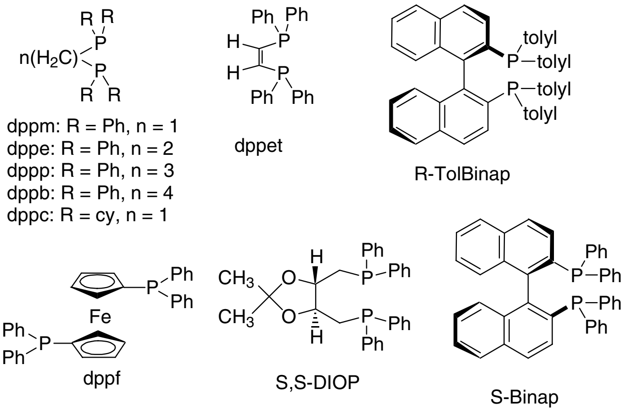

Fig. 1. Structures of the ligands employed in this work.

The interaction between bidentate diphosphines $R_2P(R')_nPR_2$ and silver salts has recently attracted a great deal of interest because the resultant complexes have found applications in homogeneous catalysis [6] and also as antitumor compounds [7]. For example silver(I) carboxylate-(S)-Binap (S-Binap = (S)-(-)-2,2′-bis(diphenylphosphino)-1,1′-binaphthyl) complexes have been recently reported as highly efficient catalysts for the Mukaiyama aldol reaction using silyl enol ethers or ketene silyl acetals as nucleophiles [8–10], this kind of catalyst strongly activating nucleophiles to undergo the aldol reaction easily. Catalytic asymmetric allylation of aldehydes using a chiral silver(I) complex has been also reported by Yamamoto and coworkers [11].

The interplay of parameters such as the geometrical flexibility of Ag(I), bite angle, electronic properties of the phosphine, and coordination mode of the supporting ligands often renders predictions concerning the structures and properties of silver-diphosphino complexes [7], both in solution and in the solid state, difficult [12,13]; to date little systematic work has been reported on the interaction between silver salts and diphosphines characterized by different spacers R′ or substituents R. The purpose of this work is to further clarify the effect of R and R′ on the coordination mode of phosphine and on the coordination environment of silver(I); we report hereunder results obtained concerning the interaction between $AgNO_2$ and the diphosphines depicted in Fig. 1, to assist our understanding of the Ag(I) species present both in solid and solution.

2. Experimental

2.1. Materials and methods

$AgNO_2$ and $R_2P(R')_nPR_2$ (dppm: $R = Ph$, $R' = CH_2$, $n = 1$; dppe: $R = Ph$, $R' = CH_2$, $n = 2$; dppp: $R = Ph$, $R' = CH_2$, $n = 3$; dppb: $R = Ph$, $R' = CH_2$, $n = 4$; dppf: $R = Ph$, $R' =$ ferrocenyl, $n = 1$; dppet: $R = Ph$, $R' = CH{=}CH$, $n = 1$; dcpm: $R = cy$, $R' = CH_2$, $n = 1$; S-Binap: $R = Ph$, $R' =$ (R)-(+)-1,1-binaphthyl, $n = 1$, $n = 2$; (R-Tol-Binap: $R = p$-tolyl; $R' =$ (R)-(+)-1,1-binaphthyl, $n = 1$; (S,S-Diop: $R = Ph$, $R' =$ (4*S*,5*S*-(+)-*O*-isopropylidene-2-3-dihydroxybutane, $n = 1$) were purchased from Aldrich and used without further purification. All reactions were carried out under an atmosphere of dry oxygen-free dinitrogen, using standard Schlenk techniques and protected from light. All solvents were dried, degassed and distilled prior to use. Elemental analyses (C, H, N) were performed with a Fisons Instruments 1108 CHNS-O Elemental analyser. IR spectra were recorded from 4000 to 100 cm^{-1} with a Perkin–Elmer System 2000 FT-IR instrument. ^1H and ^{31}P NMR spectra were recorded on a VXR-300 Varian spectrometer operating at room temperature (300 MHz for ^1H, and 121.4 MHz for ^{31}P). ^{31}P CPMAS solid-state NMR spectra were acquired at room temperature on a Bruker MSL-400 spectrometer operating at a field strength of 9.40 T (400.13 MHz for ^1H and 161.924 MHz for ^{31}P). Conventional cross-polarization and magic-angle-spinning techniques, coupled with spin temperature alternation to eliminate spectral artefacts, were implemented using a Bruker 4 mm double-air-bearing probe in which MAS frequencies of ~10 kHz were achieved. A recycle delay of 30 s, a ^1H–^{31}P contact period of 10 ms, a ^1H $\pi/2$ pulse length of 3 μs and ^1H decoupling fields of 85–90 kHz (during acquisition) were used in these measurements. No spectral smoothing was invoked prior to Fourier transformation. The 2D ^{31}P CPCOSY experiment was implemented with the TPPI (time proportional phase incrementation) method [14–16] for the acquisition of phase-sensitive data in both the F_1 and F_2 dimensions. The application of this technique has been discussed in detail elsewhere [17]. The recycle delay, contact period, ^1H $\pi/2$ pulse length and MAS rate were the same as those implemented in the above 1D ^{31}P CPMAS experiments. A total of 256 F_1 increments were acquired into 256 word blocks, with both dimensions zero-filled to 1 K words and weighted with sine-bell multiplication prior to Fourier transformation. All chemical shifts in these 1D and 2D experiments were externally referenced to 85% H_3PO_4 via solid triphenylphosphine (δ, −9.9).

The electrical resistance of CH_2Cl_2 solutions was measured with a Crison CDTM 522 conductimeter at room temperature. The positive and negative electrospray mass spectra were obtained with a Series 1100 MSI detector HP spectrometer, using an acetonitrile mobile phase. Solutions (3 mg/ml) for electrospray ionization mass spectrometry (ESI-MS) were prepared using reagent grade acetone or acetonitrile. For the ESI-MS data, masses and intensities were compared to those calculated using the IsoPro Isotopic Abundance Simulator, version 2.1) [18]. Peaks containing silver(I) ions were identified as the center of an isotopic cluster. Melting points were obtained using a Stuart SMP3 melting point apparatus and were not corrected. Molecular mass determination of compound **1** (solution) was performed at 40 °C with a Knauer KNA0280 vapor pressure osmometer calibrated with benzil. The solvent was Baker Analyzed Spectrophotometric grade chloroform. The results were reproducible to ±2%.

2.2. Syntheses

*2.2.1. Synthesis of [$(AgNO_2)_2(dppm)_3$] (**1**)*

$AgNO_2$ (0.154 g, 1 mmol) was added to a methanol solution (30 ml) of dppm (0.961 g, 2.5 mmol), at 60 °C. After the addition, the solution was stirred for 24 h at 60 °C in the dark. A colorless precipitate formed which was filtered off and washed with methanol (3 × 5 ml). Crystallization from methanol gave complex **1** as a microcrystalline solid in 68% yield. M.p. 113 °C. ^{1}H NMR ($CDCl_3$, 293 K): δ 3.3 br (2H, PCH_2P), 7.20–7.30m, 7.40–7.50m (20H, PC_6H_5). Λ_{mol} (CH_2Cl_2, concentration $= 1.00 \times 10^{-3}$ M): 7.9 $\Omega^{-1}\,cm^2\,mol^{-1}$. IR ($cm^{-1}$): 3048w [$\nu$(C–H)], 1572m [$\nu$(C=C)], 1432s, 1332m, 1310m, 1271w [ν_{asym}(NO)], 1174s br [ν_{sym}(NO)], 843m [δ(ONO)], 518s, 503s, 472s, 462s, 446m, 438m, 427w [ν(P–Ph)], 369m, 352w, 338m, 315w, 303m, 281m, 264w, 252w, 244w, 225m, 208w. ESI MS (MeCN): (+) 684 (20) $[Ag_2NO_2(dppm)]^+$, 876 (70) $[Ag(dppm)_2]^+$, 892 (25) $[Ag(dppm)_2 + O]^+$, 1030 (100) $[Ag_2NO_2(dppm)_2]^+$, 1526 (80) $[Ag_2NO_3(dppmO_2)_2]^+$. *Anal.* Calc. for $C_{75}H_{66}$-$Ag_2N_2O_4P_6$: C, 61.66; H, 4.55; N, 1.92. Found: C, 61.32; H, 4.76; N, 1.97%.

*2.2.2. Synthesis of [$AgNO_2(dppm)]_2$ (**2**)*

Compound **2** has been prepared similarly by using 1 mmol of $AgNO_2$ and 1 mmol of dppm, giving 42% yield and was recrystallized from methanol as microcrystalline solids. M.p. 205 °C. ^{1}H NMR ($CDCl_3$, 293 K): δ 3.60s (2H, PCH_2P), 7.20–7.48m, 7.44d br (20H, PC_6H_5). Λ_{mol} (CH_2Cl_2, concentration $= 1.00 \times 10^{-3}$ M): 6.7 $\Omega^{-1}\,cm^2\,mol^{-1}$. IR ($cm^{-1}$): 3078w, 3052w [$\nu$(C–H)], 1683w, 1661w [$\nu(NO_2)$], 1586w, 1573w [$\nu$(C=C)], 1436s, 1333m [$\nu_{asym}$(NO)], 1296m, 1278m, 1219sbr [ν_{sym}(NO)], 1185m, 1159m, 1129m, 860w, 845m, 838sh, 827s [δ(ONO)], 512s, 504vs, 473vs, 452m, 410m [ν(P–Ph)], 276m, 256m, 210w. ESI MS (MeCN): (+) 684 (30) $[Ag_2NO_2(dppm)]^+$, 876 (35) $[Ag(dppm)_2]^+$, 1019 (100) $[Ag_2Cl(dppm)_2]^+$, 1144 (30) $[Ag_3Cl(OH)(dppm)_2]^+$. *Anal.* Calc. for $C_{25}H_{22}AgNO_2P_2$: C, 55.79; H, 4.12; N, 2.60. Found: C, 55.51; H, 4.28; N, 2.62%.

*2.2.3. Synthesis of [$AgNO_2(dppe)]_2$ (**3**)*

$AgNO_2$ (0.154 g, 1 mmol) was added to a methanol solution (30 ml) of dppe (0.398 g, 1 mmol), at 40 °C. After the addition, the solution was stirred for 48 h at 40 °C in the dark, and then for 2 h at room temperature. A colorless precipitate formed which was filtered off and washed with methanol (3 × 10 ml). Crystallization from methanol gave complex **3** as a microcrystalline solid in 85% yield. M.p. 240 °C. ^{1}H NMR ($CDCl_3$, 293 K): δ 2.45–2.55m (4H, PCH_2CH_2P), 7.20–7.50m (20H, PC_6H_5). Λ_{mol} (CH_2Cl_2, concentration $= 1.00 \times 10^{-3}$ M): 2.4 $\Omega^{-1}\,cm^2\,mol^{-1}$. IR ($cm^{-1}$): 3070w, 3049w [$\nu$(C–H)], 1664w, 1617w [$\nu(NO_2)$], 1586w, 1572w [$\nu$(C=C)], 1435s, 1333w, 1320m [ν_{asym}(NO)], 1308m, 1277w, 1214m [ν_{sym}(NO)], 1185m, 1175s, 1158m 844w, 828m [δ(ONO)], 508vs, 482s, 474s, 464m, 418m [ν(P–Ph)], 342m, 315w, 303w, 280m, 264w, 254m, 224w, 203w. ESI MS (MeCN): (+) 905 (100) $[Ag(dppe)_2]^+$. *Anal.* Calc. for $C_{26}H_{24}AgNO_2P_2$: C, 56.54; H, 4.38; N, 2.54. Found: C, 56.34; H, 4.39; N, 2.38%.

*2.2.4. Synthesis of [$Ag(dppe)_2]NO_2$ (**4**)*

Compound **4** was prepared as for **3**, using 1 mmol of $AgNO_2$ and 2 mmol of dppe, re-crystallization from methanol giving a microcrystalline solid in 45% yield. M.p. 235 °C. ^{1}H NMR ($CDCl_3$, 293 K): δ 2.42m br (4H, PCH_2CH_2P), 7.12–7.50m, 7.65–7.75m, 7.85–7.95m (20H, PC_6H_5). Λ_{mol} (CH_2Cl_2, concentration $= 1.00 \times 10^{-3}$ M): 44.2 $\Omega^{-1}\,cm^2\,mol^{-1}$. IR ($cm^{-1}$): 3043w [$\nu$(C–H)], 1586w, 1569w, [$\nu$(C=C)], 1432m, 1303w, 1273w [ν_{asym}(NO)], 1175m, 1151m [ν_{sym}(NO)], 889m, 850m, 814w [δ(ONO)], 509vs, 477s, 462m, 440m, 430m, 418m, 400m [ν(P–Ph)], 374w, 340m, 302m, 280s, 266w, 253m, 246m, 223m, 213w. ESI MS (MeCN): (+) 905 (100) $[Ag(dppe)_2]^+$. *Anal.* Calc. for $C_{52}H_{48}AgNO_2P_4$: C, 65.69; H, 5.09; N, 1.47. Found: C, 65.66; H, 5.02; N, 1.58%.

*2.2.5. Synthesis of [$AgNO_2(dppp)]_2$ (**5**)*

Compound **5** was prepared as for **3**, using 1 mmol of $AgNO_2$ and 1 mmol of dppp, re-crystallization from methanol giving a microcrystalline solid in 54% yield. M.p. 194 °C. ^{1}H NMR ($CDCl_3$, 293 K): δ 1.75br (2H, $PCH_2CH_2CH_2P$), 2.30t (4H, $PCH_2CH_2CH_2P$), 7.20–7.50m (20H, PC_6H_5). Λ_{mol} (CH_2Cl_2, concentration $= 1.00 \times 10^{-3}$ M): 2.1 $\Omega^{-1}\,cm^2\,mol^{-1}$. IR ($cm^{-1}$): 3071w, 3045w [$\nu$(C–H)], 1661w, 1627w [$\nu(NO_2)$], 1586m, 1573w [$\nu$(C=C)], 1432s, 1417w, 1306m [ν_{asym}(NO)], 1270w, 1217sbr [ν_{sym}(NO)], 1152m, 860w, 844w, 823m [δ(ONO)], 520s, 504vs, 482s, 474s, 445m, 422w [ν(P–Ph)], 383m, 357w, 372w, 313m, 280m, 247m, 226m. ESI MS (MeCN): (+) 933 (100) $[Ag(dppp)_2]^+$. *Anal.* Calc. for $C_{27}H_{26}AgNO_2P_4$: C, 57.26; H, 4.63; N, 2.47. Found: C, 56.90; H, 4.88; N, 2.37%.

*2.2.6. Synthesis of [$AgNO_2(dppb)]_2$ (**6**)*

Compound **6** was prepared as for **3**, using 1 mmol of $AgNO_2$ and 2.5 mmol of dppb, re-crystallization from methanol giving a microcrystalline solid in 66% yield. M.p. 235 °C. ^{1}H NMR ($CDCl_3$, 293 K): δ 1.5 br (4H, $PCH_2CH_2CH_2CH_2P$), 2.0 br (4H, $PCH_2CH_2CH_2CH_2P$), 7.10–7.55m, 7.62–7.75m (20H, PC_6H_5). Λ_{mol} (CH_2Cl_2, concentration $= 1.00 \times 10^{-3}$ M): 8.3 $\Omega^{-1}\,cm^2\,mol^{-1}$. IR ($cm^{-1}$): 3073w [$\nu$(C–H)], 1626w [$\nu(NO_2)$], 1585w, 1570w [$\nu$(C=C)], 1432s, 1304m [$\nu_{asym}$(NO)], 1271w, 12130m [$\nu_{sym}$(NO)], 1178s br, 843m [$\delta$(ONO)], 516s, 510s, 478s, 456m, 445m, 409w, 397w [ν(P–Ph)], 303m, 278w, 265w, 254w, 247w, 225w, 208w. ESI MS (MeCN): (+) 961 (100) $[Ag(dppb)_2]^+$, 977 (50) $[Ag(dppb)_2+(O)]^+$. *Anal.* Calc. for $C_{52}H_{48}AgNO_2P_4$: C, 65.69; H, 5.09; N, 1.47. Found: C, 65.66; H, 5.39; N, 1.56%.

2.2.7. Synthesis of $[AgNO_2(dppf)]_2$ (7)

Compound **7** was prepared as for **3** using 1 mmol of $AgNO_2$ and 2.5 mmol of dppf, re-crystallization giving a microcrystalline solid in 80% yield. M.p. 221 °C. ^1H NMR ($CDCl_3$, 293 K): δ 4.20–4.40m (8H, C_5H_5), 7.20–7.50m, 7.55–7.70m (20 H, PC_6H_5). Λ_{mol} (CH_2Cl_2, concentration = 1.00×10^{-3} M): 1.2 $\Omega^{-1}\,cm^2\,mol^{-1}$. IR ($cm^{-1}$): 3052w [$\nu$(C–H)], 1662w, 1646w [$\nu(NO_2)$], 1586w, 1571w [$\nu$(C=C)], 1434s, 1312m [$\nu_{asym}$(NO)], 1227m [$\nu_{sym}$(NO)], 1196m, 1180m, 1170s, 1160m, 885w, 868w, 835m, 828m [δ(ONO)], 536s, 513vs, 490vs, 470s, 456s, 432m, 420m, 399w [ν(P–Ph)], 375w, 352m, 327w, 314w, 304w, 283w, 278m, 267w, 253w, 246m, 228w, 223w, 212w. ESI MS (MeCN): (+) 662 (40) $[Ag(dppf)]^+$, 1216 (100) $[Ag(dppf)_2]^+$, 1232 (20) $[Ag(dppf)_2+(O)]^+$. *Anal.* Calc. for $C_{34}H_{28}AgFeNO_2P_2$: C, 57.66; H, 3.98; N, 1.98. Found: C, 57.43; H, 4.02; N, 1.82%.

2.2.8. Synthesis of $[(AgNO_2)_2(dppet)]_2$ (8)

Compound **8** was prepared as for **3**, using 1 mmol of $AgNO_2$ and 1 mmol of dppet in dichloromethane, re-crystallization from methanol giving a microcrystalline solid in 62% yield. M.p. 170 °C. ^1H NMR ($CDCl_3$, 293 K): δ 7.22–7.44m (22H, PC*H*=C*H*P and PC_6H_5). Λ_{mol} (CH_2Cl_2, concentration = 1.00×10^{-3} M): 0.9 $\Omega^{-1}\,cm^2\,mol^{-1}$. IR ($cm^{-1}$): 3182w [$\nu$(C–H)], 1684w, 1653w [$\nu(NO_2)$], 1576w [$\nu$(C=C)], 1303m [$\nu_{asym}$(NO)], 1208 [$\nu_{sym}$(NO)], 1155m br, 890m, 844w [δ(ONO)], 556vs, 514s, 500w, 482m, 470w, 461m, 433m, 406w [ν(P–Ph)], 371w, 352m, 326w, 315w, 290w, 281w. ESI MS (MeCN): (+) 1467 (100) $[Ag_2(NO_2)(dppet)_3+(O)]^+$. *Anal.* Calc. for $C_{26}H_{22}Ag_2N_2O_4P_2$; C, 44.35; H, 3.15; N, 3.98. Found: C, 44.73; H, 3.22; N, 3.80%.

2.2.9. Synthesis of $[AgNO_2(dcpm)]_2$ (9)

Compound **9** was prepared as for **8**, using 1 mmol of $AgNO_2$ and 1 mmol of dcpm in dichloromethane, re-crystallization from methanol giving a microcrystalline solid in 57% yield. M.p. 259 °C. ^1H NMR ($CDCl_3$, 293 K): δ 1.15–1.40m (22H, PC_6H_{11}), 1.68s (2H, PCH_2P), 1.73–1.9m (22H, PC_6H_{11}). Λ_{mol} (CH_2Cl_2, concentration = 1.00×10^{-3} M): 0.9 $\Omega^{-1}\,cm^2\,mol^{-1}$. IR ($cm^{-1}$): 1651w, 1644w [$\nu(NO_2)$], 1447s, 1366m, 1350m, 1327m [ν_{asym}(NO)], 1295m, 1215m [ν_{sym}(NO)], 1188s, 1175s, 1149m 887m, 848s, 819m [δ(ONO)], 517s br, 492s br, 471s, 459s, 419m, 398m, 385w, 375w, 351m, 341w, 326w, 303m, 282w, 278w, 267w, 248m, 229m, 221w. ESI MS (MeCN): (+) 1078 (100) $[Ag_2(NO_2)(dcpm)_2]^+$. *Anal.* Calc. for $C_{25}H_{46}AgNO_2P_2$: C, 53.39; H, 8.24; N, 2.49. Found: C, 53.10; H, 8.35; N, 2.32%.

2.2.10. Synthesis of $[AgNO_2(R)$-Tol-Binap)] (10)

Compound **10** was prepared as for **3**, using 1 mmol of $AgNO_2$ and 1 mmol of R-Tol-Binap in dichloromethane, re-crystallization from methanol giving a microcrystalline solid in 68% yield. M.p. 252 °C. ^1H NMR ($CDCl_3$, 293 K): δ 1.72s, 1.90s, 2.34s, 2.46s (12H, $CH_3C_6H_4P$), 5.80d, 6.24d, 6.76d, 6.91q, 7.01t, 7.15–7.28m, 7.43d, 7.46d, 7.69q (28H, $H_{aromatic}$ of R-Tol-Binap). Λ_{mol} (CH_2Cl_2, concentration = 1.00×10^{-3} M): Λ 0.8 $\Omega^{-1}\,cm^2\,mol^{-1}$. IR ($cm^{-1}$): 3065w [$\nu$(C–H)], 1587w, 1575w [$\nu$(C=C)], 1390m, 1337m, 1303m [ν_{asym}(NO)], 1216s br [ν_{sym}(NO)], 1179m, 1087m, 869m, 840m, 808s [δ(ONO)], 516sh, 511vs, 497s, 470m, 444m, 428m, 404w, 398m [ν(P–Ph)], 352m, 324w, 302w, 279m, 246w, 223m. ESI MS (MeCN): (+) 1465 (100) $[Ag(R\text{-}Tol\text{-}Binap)_2]^+$. *Anal.* Calc. for $C_{48}H_{40}AgNO_2P_2$: C, 69.24; H, 4.84; N, 1.68. Found: C, 68.93; H, 4.98; N, 1.42%.

2.2.11. Synthesis of $[Ag(NO_2)$(S-Binap)] (11)

Compound **11** was prepared as for **3**, using 1 mmol of $AgNO_2$ and 1 mmol of S-Binap in dichloromethane, re-crystallization from methanol giving a microcrystalline solid in 77% yield. M.p. 134 °C. ^1H NMR ($CDCl_3$, 293 K): 5.98t, 6.49t, 6.67t, 6.77d, 7.00–7.20m, 7.29t, 7.48–7.60m, 7.62–7.90m (32H, $H_{aromatic}$ of S-Binap). Λ_{mol} (CH_2Cl_2, concentration = 1.00×10^{-3} M): 0.9 $\Omega^{-1}\,cm^2\,mol^{-1}$. IR ($cm^{-1}$): 3075w [$\nu$(C–H)], 1584w, 1549w [$\nu$(C=C)], 1432s, 1340m, 1303w, 1275w [ν $_{asym}$(NO)], 1220m [ν_{sym}(NO)], 1158m, 1148m, 1089m, 870m, 816s [δ(ONO)], 540m, 520s, 506vs, 494s, 450m, 431m, 419w, 398m [ν(P–Ph)], 375w, 352w, 329w, 290m, 280m, 266w, 245w. ESI MS (MeCN): (+) 1353 (100) $[Ag(S\text{-}BINAP)_2]^+$, 1369 (20) $[Ag(S\text{-}Binap)_2+(O)]^+$, 1507(3) $[Ag_2(NO_2)(S\text{-} Binap)_2]^+$. *Anal.* Calc. for $C_{44}H_{32}AgNO_2P_2$: C, 68.05; H, 4.15; N, 1.80. Found: C, 68.35; H, 4.28; N, 1.62%.

2.2.12. Synthesis of $[Ag(NO_2)$(SS-Diop)] (12)

Compound **12** was prepared as for **3**, using 1 mmol of $AgNO_2$ and 1 mmol of S,S-diop in dichloromethane, re-crystallization from methanol giving a microcrystalline solid in 63% yield. M.p. 128 °C. ^1H NMR ($CDCl_3$, 293 K): δ 1.30s (6H, CH_{3DIOP}), 2.44dd, 86br (4H, CH_2P_{Diop}), 4.18br (2H, O–CH_{Diop}), 7.22–7.50m, 7.56–7.82m (20H, $H_{aromatic}$ of S,S-Diop). Λ_{mol} (CH_2Cl_2, concentration = 1.00×10^{-3} M): 0.9 $\Omega^{-1}\,cm^2\,mol^{-1}$. IR ($cm^{-1}$): 3072w, 3048w [$\nu$(C–H)], 1658w, 1627w [$\nu(NO_2)$], 1585w, 1573w [$\nu$(C=C)], 1438s, 1339m, 1307m [ν_{asym}(NO)], 1221m [ν_{sym}(NO)], 1212sbr, 1186m, 1174s, 1156m 884s, 846w, 832w [δ(ONO)], 5068vs, 472s, 437m, 418m [ν(P–Ph)], 347m, 312w, 281w, 264w, 247m, 226m, 211w. ESI MS (MeCN): (+) 1105 (100) $[Ag(S,S\text{-}Diop)_2]^+$, 1121 (25) $[Ag(S,S\text{-}Diop)_2+O]^+$ 1258 (10) $[Ag_2(NO_2)(S,S\text{-}Diop)_2]^+$. *Anal.* Calc. for $C_{31}H_{32}AgNO_2P_2$: C, 57.07; H, 4.94; N, 2.15. Found: C, 57.43; H, 5.06; N, 2.02%.

Table 1
$^{31}P\{^1H\}$ NMR data of compounds **1**–**12** ($CDCl_3$)

Compound	$\delta(^{31}P)^a$ 295 K	$^1J(^{31}P–Ag)^b$	$\delta(^{31}P)$ 218 K	$^1J(^{31}P–Ag)$	$\delta(^{31}P)_{freeP-donor}$	Δ^c
1	−6.5br		5.35d	479	−21.5	15
			−3.0d br			
			−11.95d	220		
			−23.7s br			
2	4.29dt	462	5.11dm	470	−21.5	25.8
	4.3br					
3	5.3br		6.59d	442	−12.0	17.3
			5.17d	445		
4	3.2dbr	242	5.77dbr	249	−12.0	15.2
5	1.5br		0.51dd	413 (^{107}Ag)	−16.8	18.3
				477 (^{109}Ag)		
6	0.3br		1.9d	418	−15.5	15.8
			−1.5d	405		
7	−3.9dbr		−4.09dd	387 (^{107}Ag)	−16.8	12.9
				447 (^{109}Ag)		
8	−8.04br		4.21	255	−22.8	14.8
			−7.59	718		
9	21.1dt	461	19.8dm	463	−9.5	30.6
10	13.0dd	239	14.1dd	380 (^{107}Ag)	−11.5br	24.5
				438 (^{109}Ag)		23.1
	11.6d br		13.9dd	225 (^{107}Ag)		
				258 (^{109}Ag)		
11	15.8d	241	16.9dd	224.0–258.2	−15.2	31.0
	12.9d	360	15.2dd	343–394		28.1
12	−9.7dbr	372	−9.8d	406	−23.0	13.3
			−9.7d	407		

[a] δ in ppm.
[b] J in Hz.
[c] $\Delta = \delta(^{31}P)_{complex} - \delta(^{31}P)_{freeP}$.

2.3. X-ray crystallographic studies

Full spheres of CCD area detector diffractometer data were measured (Bruker AXS instrument, ω-scans; monochromatic Mo Kα radiation, $\lambda = 0.7107_3$ Å; T ca. 153 K) yielding $N_{t(otal)}$ reflections, merging to N unique (R_{int} cited) after 'empirical'/multiscan absorption correction (proprietary software), N_o being considered 'observed' and used in the full matrix least squares refinements. Anisotropic displacement parameter forms were refined for the non-hydrogen atoms, $(x, y, z, U_{iso})_H$ being included, constrained at estimates. Conventional residuals R, R_w (weights: $(\sigma^2(F) + 0.0004F^2)^{-1}$) are cited on $|F|$ at convergence. Neutral atom complex scattering factors were employed within the XTAL 3.7 program system [19]. Pertinent results are given below and in Tables 3–6 and Figs. 8–11, the latter showing 50% probability amplitude displacement envelopes for the non-hydrogen atoms, hydrogen atoms having arbitrary radii of 0.1 Å. CCDC 219656–219659.

Table 2
^{31}P CPMAS NMR data[a]

Compound	$\delta(^{31}P)^b$	$^1J(^{31}P–Ag)^c$
1	12.52m	439
	−0.81m	478
	−24.95m	370
2	−4.19	444
5	7.05d	488
	7.12d	449
6	−0.87d	439
7	−1.29	440
8	−0.10br	
	−12.63d	683
9	30.25d	469
	21.68d	498
10	1.12br	
	−2.01br	
	−5.03br	
$AgNO_3$:dppm (1:1)	7.0m	498
	0.70m	459

[a] (v_r = 10 KHz).
[b] δ in ppm.
[c] J in Hz.

3. Results and discussion

3.1. Syntheses

The reaction of $AgNO_2$ with 2.5 equiv of bis(diphenylphosphino)methane (dppm) in methanol at 60 °C gave rise to compound **1** $[Ag_2(dppm)_3](NO_2)_2$ which presumably is analogous to the structurally characterized $[Ag_2(dppm)_3](NO_3)_2$ (Fig. 2(a)) [20]. When the

Table 3
Crystal/refinement data

Compound	**2**[a]	**5**	**8**[b]	**10**[c]
	$AgNO_2$:$(Ph_2P)_2CH_2$ $(1:1)_2 \cdot$ MeOH	$AgNO_2$:$(Ph_2PCH_2)_2CH_2$ $(1:1)_2$	$AgNO_2$:$(Ph_2PCH)_2$ $(2:1)_2$	$AgNO_2$:(*p*-tol$_2$ $P(C_{10}H_6)_2)_2$ (1:1)
Formula	$C_{52}H_{52}Ag_2N_2O_6P_4$	$C_{54}H_{52}Ag_2N_2O_4P_4$	$C_{52}H_{44}Ag_4N_4O_8P_4$	$C_{48}H_{40}AgNO_2P_2$
M_r	1140.6	1132.7	1408.3	832.7
Crystal system	monoclinic	triclinic	monoclinic	triclinic
Space group	$P2_1/n$ (C_{2h}^5, No. 14)	$P\bar{1}$ (C_i^1, No. 2)	$P2_1/n$	$P\bar{1}$ (C_1^1, No. 1)
a (Å)	11.2048(8)	10.530(1)	12.2451(7)	11.2603(8)
b (Å)	19.651(1)	10.738(1)	10.4164(6)	13.3239(9)
c (Å)	11.2534(8)	12.850(2)	20.025(1)	14.945(1)
α (°)		114.041(2)		64.916(2)
β (°)	99.218(2)	90.180(2)	91.932(2)	76.980(2)
γ (°)		110.180(2)		73.861(2)
V (Å^3)	2446	1228	2553	1936
D_c (g cm^{-3})	1.54_9	1.53_1	1.83_2	1.42_5
Z	2 dimers	1 dimer	2 f.u.	2
μ_{Mo} (mm^{-1})	0.98	0.98	1.7	0.65
Specimen (mm^3)	$0.16 \times 0.11 \times 0.07$	$0.35 \times 0.22 \times 0.15$	$0.55 \times 0.25 \times 0.025$	$0.25 \times 0.16 \times 0.10$
'T'$_{min/max}$	0.88	0.89	0.73	0.86
$2\theta_{max}$(°)	68	58	75	58
N_t	51,470	14,342	53,361	39,753
N (R_{int})	9986 (0.070)	5999 (0.023)	13,313 (0.060)	9024 (0.027)
N_o	6251	4875	8290	7823
R	0.048	0.047	0.042	0.048
R_w	0.050	0.053	0.042	0.056

[a] Difference map residues were modelled in terms of methanol of solvation, the oxygen disordered over a pair of sites, occupancies set at 0.5 after trial refinement. Associated hydrogen atoms were not located.

[b] $(x, y, z, U_{iso})_H$ were refined.

[c] High displacement parameters/disorder were evident in the two nitrite groups; disorder was resolved and refined in the N, O(1) component of nitrite 1, occupancies set at 0.5 after trial refinement, with isotropic displacement parameter forms. 'Friedel' data were preserved distinct, x_{abs} refining to −0.03(3), the chirality as shown in Fig. 2 the same for the two independent molecules in the asymmetric unit and consistent with that expected for the ligand as supplied.

Table 4
Selected geometries, $AgNO_2$:(*p*-tolyl$_2$P$(C_{10}H_6)_2$P*p*-tolyl$_2$) (1:1) (**10**)

Atoms	Parameter	Atoms	Parameter
Bond distances (Å)			
Ag(*n*)–P(*n*1)	2.426(3), 2.438(2)	Ag(*n*)–O(*n*1)	2.31(2)[a], 2.35(1)
Ag(*n*)–P(*n*2)	2.490(2), 2.455(3)	Ag(*n*)–O(*n*2)	2.40(2), 2.39(1)
Bond angles (°)			
P(*n*1)–Ag(*n*)–P(*n*2)	96.00(8), 99.07(9)	P(*n*2)–Ag(*n*)–O(*n*1)	119.6(4)[a], 121.2(2)
P(*n*1)–Ag(*n*)–O(*n*1)	139.1(4)[a], 139.0(2)	P(*n*2)–Ag(*n*)–O(*n*2)	111.4(3), 118.2(3)
P(*n*1)–Ag(*n*)–O(*n*2)	132.8(3), 119.3(2)	O(*n*1)–Ag(*n*)–O(*n*2)	54.2(5)[a], 49.9(3)
Ag(*n*)–P(*n*1)–C(*n*112)	104.8(3), 102.6(2)	Ag(*n*)–P(*n*2)–C(*n*212)	108.8(2), 107.1(3)
Ag(*n*)–P(*n*1)–C(*n*121)	116.4(4) 113.3(3)	Ag(*n*)–P(*n*2)–C(*n*221)	117.0(3), 113.9(4)
Ag(*n*)–P(*n*1)–C(*n*131)	115.7(3), 123.3(2)	Ag(*n*)–P(*n*2)–C(*n*231)	113.6(3, 115.5(3)
C(*n*112)–P(*n*1)–C(*n*121)	104.2(4), 106.2(4)	C(*n*212)–P(*n*2)–C(*n*222)	107.4(4), 105.0(4)
C(*n*112)–P(*n*1)–C(*n*131)	107.7(4), 104.0(5)	C(*n*212)–P(*n*2)–C(*n*232)	106.6(4), 106.0(5)
C(*n*121)–P(*n*1)–C(*n*131)	107.1(4), 105.8(4)	C(*n*222)–P(*n*2)–C(*n*232)	102.7(4), 108.5(4)
Torsion angles (°) (carbon atoms denoted by number only)			
Ag(*n*)–P(*n*1)–*n*112–*n*111	76.4(9), 73.4(7))	Ag(*n*)–P(*n*2)–*n*212–*n*211	68.3(6), 66.0(8)
Ag(*n*)–P(*n*1)–*n*121–*n*122	–11.2(7), 35.3(9)	Ag(*n*)–P(*n*2)–*n*211–*n*222	−19.3(7), 21.4(9)
Ag(*n*)–P(*n*1)–*n*131–*n*132	4.0(6), 8.5(10)	Ag(*n*)–P(*n*2)–*n*231–*n*232	11(1), 10.4(7)
*n*112–*n*111–*n*211–*n*212	−77(1), −83(1)		

The two values in each entry are for molecules 1,2.

[a] Ag(1)–O(11′) is 2.42(2) Å; P(11,12)–Ag–O(11′) are 143.7(3), 119.9(3) and O(12)–Ag–O(11′) 41.0(5)°.

reaction between $AgNO_2$ and dppm was carried out with a 1:1 ligand to metal ratio, the dinuclear compound $[Ag_2(dppm)_2(NO_2)_2]$ **2** formed (Fig. 2(b)) (see below, X-ray discussion). 1,2-Bis(diphenylphosphino)ethane (dppe) forms both 1:1 (**3**) and 2:1 (**4**) adducts depending on the ligand stoichiometry employed. Only 1:1 adducts

Table 5
Selected geometries, AgNO$_2$:(Ph$_2$P(CH$_2$)$_n$PPh$_2$) (1:1)$_2$ ($n = 1, 3$) (**2** and **5**)

Atoms	Parameter	Atoms	Parameter
Bond distances (Å)			
Ag–P(1)	2.4346(9), 2.422(1)	Ag–O(1)	2.694(4), 2.559(5)
Ag–P(2′)	2.4536(9), 2.450(1)	Ag–O(2)	2.475(3), 2.481(7)
Ag···Ag′	3.1877(4), 4.5737(9)	Ag···O(1′)	4.311(4), 3.127(4)
		O(1)···O(1′)	6.444(5), 3.426(7)
Bond angles (°)[b]			
P(1)–Ag–P(2′)	148.28(3), 143.67(4)	P(2′)–Ag–O(1)	82.99(8), 100.3(1)
P(1)–Ag–O(1)	127.90(8), 113.3(1)	P(2′)–Ag–O(2)	99.33(8), 100.9(2)
P(1)–Ag–O(2)	107.24(8), 112.2(2)	O(1)–Ag–O(2)	47.9(1), 45.6(2)
Ag–P(1)–C(1)	113.6(1), 111.7(2)	Ag′–P(2)–C(1,2)	108.2(1), 107.5(1)
Ag–P(1)–C(111)	116.0(1), 115.8(2)	Ag′–P(2)–C(211)	119.8(1), 117.8(2)
Ag–P(1)–C(121)	113.0(1), 115.5(1)	Ag′–P(2)–C(221)	114.8(1), 118.3(1)
C(1)–P(1)–C(111)	104.0(2), 104.6(2)	C(1,2)–P(2)–C(211)	103.9(2), 104.4(2)
C(1)–P(1)–C(121)	103.8(2), 100.8(2)	C(1,2)–P(2)–C(221)	103.1(9), 102.9(2)
C(111)–P(1)–C(121)	105.2(2), 106.9(2)	C(211)–P(2)–C(221)	105.2(2), 104.1(2)
P(1)–C(1)–P(2)	110.1(2)		
Torsion angles (°) (carbon atoms denoted by number only)			
Ag–P(1)–1–P(2),12	−33.6(2), −42.7(3)	Ag′–P(2)–1,2–P(1),12	68.6(2), 59.7(3)
Ag–P(1)–111–112	−5.0(3), −0.5(3)[a]	Ag′–P(2)–211–212	−1.2(3), 17.7(4)
Ag–P(1)–121–122	−68.7(3), −58.2(3)[a]	Ag′–P(2)–221–222	65.8(3), 67.0(5)

Primed atoms are inversion related; the two values in each entry are for $n = 1, 3$, respectively.

[a] For 112 read 116.

[b] In **5**, angles C(1,12,2) are 112.9(3)°, 111.9(4)°, 110.3(3)°.

Table 6
Selected geometries, AgNO$_2$:(Ph$_2$PCH:CHPPh$_2$) (2:1)$_2$ (**8**)

Atoms	Parameter	Atoms	Parameter
Bond distances (Å)			
Ag(1)–P(1)	2.3651(7)	Ag(2)–P(2)	2.3786(7)
Ag(1)–O(11)	2.332(2)	Ag(2)–O(12)	2.249(3)
Ag(1)–O(21′)	2.286(2)	Ag(2)–O(21)	2.426(2)
N(1)–O(11)	1.239(4)	Ag(2)–O(22)	2.522(2)
N(1)–O(12)	1.259(4)	N(2)–O(21)	1.275(3)
Ag(2)···Ag(2′)	3.7923(4)	N(2)–O(22)	1.233(3)
C(1)–C(2)	1.337(4)	Ag(1)···Ag(2)	2.8463(3)
Bond angles (°)			
P(1)–Ag(1)–O(11)	122.36(7)	P(2)–Ag(2)–O(12)	150.97(7)
P(1)–Ag(1)–O(21′)	146.59(5)	P(2)–Ag(2)–O(21)	121.28(5)
O(11)–Ag(1)–O(21′)	90.90(8)	P(2)–Ag(2)–O(22)	112.30(6)
Σ	359.8$_5$	O(12)–Ag(2)–O(21)	87.64(8)
Ag(1)–O(11)–N(1)	123.5(2)	O(12)–Ag(2)–O(22)	83.39(8)
Ag(2)–O(12)–N(1)	136.4(2)	O(21)–Ag(2)–O(22)	50.09(7)
O(11)–N(1)–O(12)	116.1(3)	Ag(2)–O(21)–N(2)	100.0(2)
O(21)–N(2)–O(22)	113.4(2)	Ag(2)–O(21)–Ag(1′)	145.57(7)
N(2)–O(21)–Ag(1′)	113.7(2)	P(1)–C(1)–C(2)	126.5(1)
Ag(2)–O(22)–N(2)	96.5(2)	P(2)–C(2)–C(1)	125.6(2)

Primed atoms are inversion related.

(**5**–**7**, **9**) between AgNO$_2$ and 1,3-bis(diphenylphosphino)propane (dppp), 1,4-bis(diphenylphosphino)butane (dppb), 4,4′-bis(diphenylphosphino)ferrocene (dppf) or bis(dicyclohexylphosphino)methane (dcpm), have been obtained, respectively, independently of reaction conditions and ligand-to-metal ratio employed. The chiral ligands R-Tol-Binap, S,S-Binap and S,S-Diop also form 1:1 adducts (**10**–**12**), all probably possessing a mononuclear structure (Fig. 2(c)). The *cis*-1,2-bis(diphenylphosphino)ethylene ligand (dppet) is the only donor molecule which forms a tetranuclear adduct (**8**) adduct having a 1:2 ligand to metal ratio.

The complexes **1**–**6**, and **9** are air-stable, colorless materials, soluble in polar solvents such as acetonitrile, dimethylformamide and dimethylsulfoxide. They are, however, insoluble in water, ether and tetrahydrofuran but exhibit good solubility in the chlorinated hydrocarbons CH$_2$Cl$_2$ and CHCl$_3$. Solid samples and

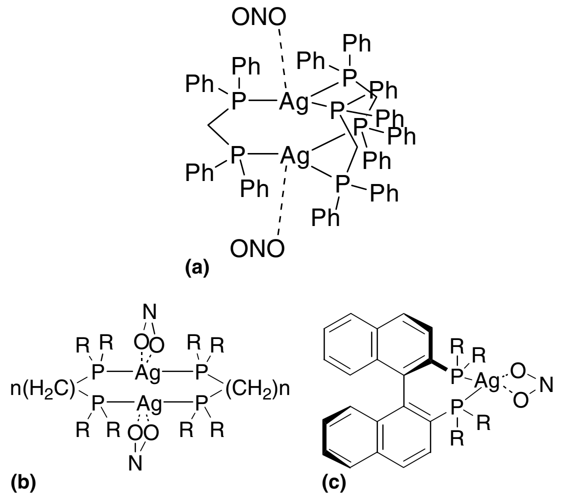

Fig. 2. Molecular Structure of compounds **2** (a), **9** (b) and **10**.

solutions of these compounds show no sensitivity to light. Compounds **7**, **8**, **10**–**12** are generally unstable in solution, their chlorinated solvent solutions often darkening in a very short time. Derivatives **10**–**12** exhibit also high sensitivity to light.

3.2. Spectroscopy

The infrared spectra of **1**–**12** (see Section 2) are consistent with the formulations proposed, showing all of the bands required by the presence of the nitrito group and of the phosphorus donor [21–24]. In some cases in the complexes the bands due to the phosphine ligands, only slightly shifted with respect to those of the free donors, are not resolved due to the presence of the very intense nitrite band in the same region. In the far-IR spectra of all derivatives **1**–**12** we assigned, on the basis of a previous report on phosphino silver(I) derivatives [25], the broad absorptions near 500 cm^{-1} and those at 450–400 cm^{-1} to Whiffen's *y* and *t* vibrations, respectively. Some bands in the region 400–300 cm^{-1}, similar to those described in the literature for triphenylphosphine silver(I) nitrate derivatives [25], can be tentatively assigned to ν(Ag–P) and ν(Ag–O) vibrations.

In the spectra of our compounds **2**, **3**, **5**–**12** the absorptions due to ν_{asym} and ν_{sym} fall in the range 1330–1290 and 1220–1200 cm^{-1}, respectively, as expected for an *O*,*O*′-chelating NO_2 group. However it has been previously proposed that the two metal–oxygen distances of a chelated nitrite can differ significantly, the detectable effect being the splitting of the sharp peak due to $\delta(NO_2)$ and a widening of the energy separation between ν_{asym} and ν_{sym} [26,27]. Both effects have been observed in our compounds, the lower separation between ν_{asym} and ν_{sym} and non-splitting of $\delta(NO_2)$ being found for the derivative **10** also, in accordance with the X-ray data (see below). The spectrum of compound **8** is more complex in accordance with the NO_2-coordination as depicted in Fig. 3. Conductivity measurements in CH_2Cl_2 confirm the ionic nature of **4**, whereas the lack of conductivity found in CH_2Cl_2 for adduct **1** is explicable with the occurrence of equilibria such as (*1*), also supported from the ^{31}P NMR solution data (see below).

$$\underset{\mathbf{1}}{[Ag_2(dppm)_3](NO_2)_2} \rightleftarrows \underset{\mathbf{2}}{[Ag_2(NO_2)_2(dppm)_2]} + dppm \qquad (1)$$

In the ^{1}H NMR spectra of **1**–**12** in $CDCl_3$ (see Section 2), the signals due to the diphosphine show a different pattern with respect to those found for the free donors, confirming the existence, at least partial, of the complexes in solution. The bridging methylene resonances in **1**–**6** and **9** appear as a broad singlet or multiplet between 2.50 and 3.60 ppm downfield shifted with respect to those found in the free donors.

^{31}P chemical shifts ($CDCl_3$ solution) and ^{31}P–Ag coupling-constants for derivatives **1**–**12**, are reported in Table 1. They have been found to be slightly dependent on the dilution of the solutions. Our experiments have been carried out at a concentration of 0.005 mol/L. The room temperature ^{31}P NMR spectra of complexes **3**, **5**, **6** and **8** consist of broad singlets, presumably in consequence of exchange equilibria that are reasonably fast in relation to the NMR time scale. Exchange is quenched at low temperature (218–223 K), and one and/or two unresolved doublets or resolved pairs of doublets, arising from coupling between the phosphorus and silver atom, are observed in the accessible temperature range. In particular, in the spectrum of derivative **5** typical pairs of doublets, due to $^{1}J(^{31}P–^{107}Ag)$ and $^{1}J(^{31}P–^{109}Ag)$ coupling, are resolved at 218 K and the observed $^{1}J(^{107}Ag)/^{1}J(^{109}Ag)$ ratio is in good agreement with that calculated from the gyromagnetic ratio of the Ag nuclei $\gamma(^{107}Ag)/\gamma(^{109}Ag)$ [28]. For derivatives **7** and **12** such doublets were also observed at room temperature, suggesting that rapid exchange equilibria are not operative in the cases of sterically hindered phosphines such as dppf and S,S-Diop. The signal due to each free phosphine is always up-field with respect to that of the

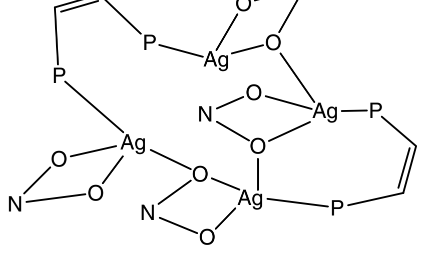

Fig. 3. Silver coordination environment in compound **8**.

corresponding silver(I) complex. The magnitudes of Δ ($\Delta = \delta^{31}P_{complex} - \delta^{31}P_{free\ ligand}$) and the coupling constants decrease with the decreasing basicity, also correlating with steric bulk and bite of the ligands. It is worthy of note that the presence of two different doublets having the same ^{31}P-Ag coupling constants in the case of compounds **3**, **6** and **12**, suggests the existence of different isomers or species in solution. Muetterties and Alegranti [29] and Goel and Pilon [30] indicated that the spin–spin constant (*J*) between phosphorus and silver changes, depending on the number of coordinated phosphorus atoms in the silver complex, and that it is possible to determine the number of the latter from measurement of the *J* values in the ^{31}P NMR spectra. On the basis of the detected values, an AgP_2O_2 coordination environment is likely in solution for compounds **3**, **5**–**8** and **12**, consistent with the structures found in the solid state. The ^{31}P NMR spectra of the R-Tol-Binap and S,S-Binap compounds **10** and **11** exhibit two double doublets, the peaks having the same intensities both at low and room temperature. We have compared our data with those reported by Yamagishi for $Ag(PF_6)$(S-Binap) systems [31]. The signals at 13.9 and 16.9 ppm in the low temperature spectra of **10** and **11** respectively can be assigned to a silver center presumably four-coordinated by a pairs of Binap ligands, whereas those at 14.1 (**10**) and 15.2 (**11**), for which greater ^{1}J(Ag–P) coupling constants were detected, could arise from a silver coordinated by two phosphorus atoms as in the solid state (see below). This means that the presence of an anion more coordinating with respect to PF_6 can modify the concentration in solution of those species active toward the Mukaiyama aldol reaction [8–10]. Molecular weight measurements carried out for compound **2** indicate the existence of **2** as a dinuclear species also in $CHCl_3$ solution, *r* (= ratio between experimental and calculated formula weight) being 1.96 at 10^{-2} m. The ^{31}P NMR spectra of compounds **2** and **9** support this finding. A double triplet and a broad signal have been found at room temperature (Fig. 4(a)), whereas the low temperature ^{31}P spectrum consists of an $AA'XX'A''A^*$ pattern (Fig. 4(b)) [32] due to the non-equivalence of the phosphorus atoms (as emerges also from the X-ray data) and resulting from the large ^{2}J(P–P), for the three possible combinations of the two silver isotopes. It is very interesting that the same pattern, differ from that previously reported [20], has been found by us also for the well known $[Ag_2(dppm)_2(NO_3)_2]$ species. The ^{31}P NMR spectrum of **1** confirms the occurrence of equilibrium (**1**), four different signals being detected at low temperature, the first due to free dppm, the second unambiguously assignable to compound **2** and a third due to a silver center coordinated by only one phosphorus atom. Finally the ^{31}P NMR spectrum of **4** is in accordance with a tetrahedral silver center four-coordinated, presumably by a pair of chelating dppe ligands, the ^{1}J(Ag–P) coupling constant being in the range typical for AgP_4 cores [29,30].

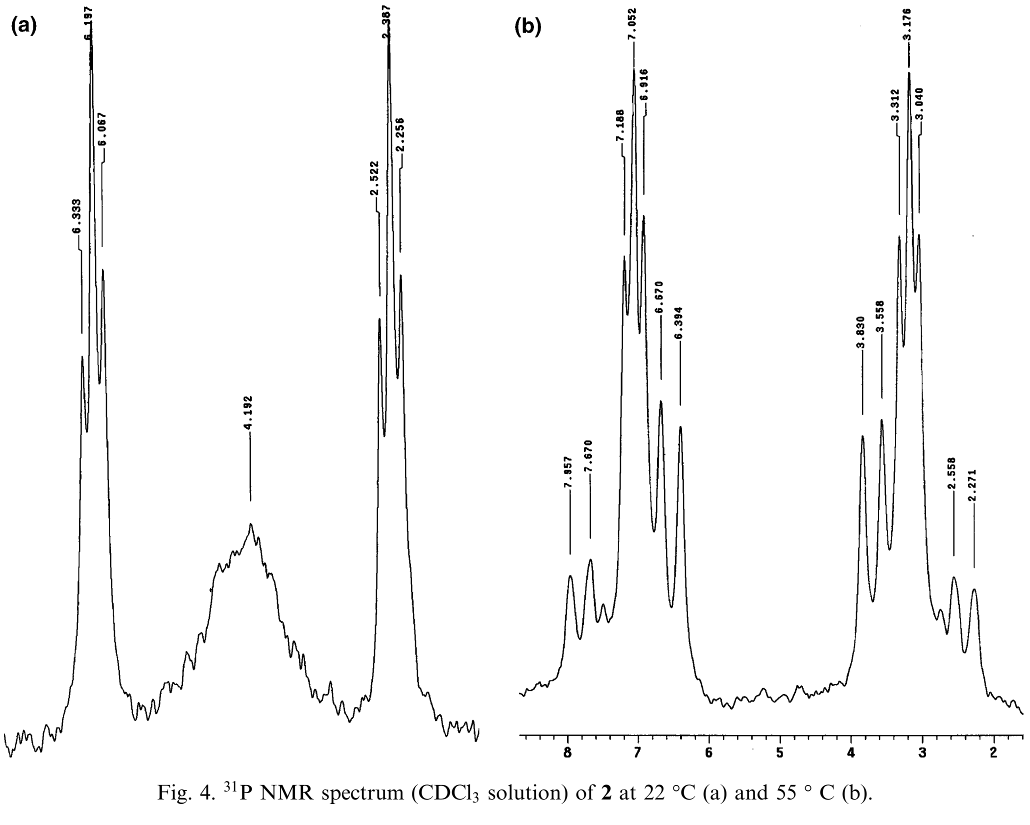

Fig. 4. ^{31}P NMR spectrum ($CDCl_3$ solution) of **2** at 22 °C (a) and 55 ° C (b).

The solid state 1D ^{31}P CPMAS and 2D ^{31}P CPCOSY NMR spectra are shown in Figs. 5 and 6, respectively. The isotropic chemical shifts and ^1J(Ag–P) heteronuclear coupling constants measured for this suite of complexes are given in Table 2. From Fig. 5(a) and (b), the P positions in the dimeric complexes [AgNO$_2$-(dppb)]$_2$ (**6**) and [AgNO$_2$(dppf)]$_2$ (**7**) are equivalent, thus giving rise to a single well-resolved doublet in each case. The measured ^1J(Ag–P) coupling constants are 439 and 449 Hz, respectively. This symmetry is somewhat lower for the [AgNO$_2$(dppm)]$_2$ (**2**) dimer, where a marked reduction in resolution is exhibited in the solid state (see Fig. 5(c)). Although, doublet structure is evident with a ^1J(Ag–P) value of ~444 Hz, it is much broader than that observed for **6** and **7** and is consistent with the AA′XX′A″A* spin system elucidated from the above ^{31}P solution NMR studies. A further reduction in symmetry is observed for the [AgNO$_2$-(dppp)]$_2$ (**5**) dimer, where Fig. 5(d) exhibits a partially resolved (overlapping) doublet structure. This is corroborated by the corresponding 2D ^{31}P CPCOSY spectrum of Fig. 6(a) which shows the two partially resolved doublets as clearly resolved correlations, one above and one below the main diagonal with ^1J(Ag–P) values of ~488 Hz (low field) and ~449 Hz (high field). These correlations are poorly formed and are indicative of an overall reduction in symmetry as experienced with tightly coupled AA′XX′A″A* or AA′XX′BB′ spin systems.

The 1D ^{31}P CPMAS spectrum of the dimeric complex [AgNO$_2$(dcpm)]$_2$ (**9**) shown in Fig. 5(e) is a well-resolved example of an AA′XX′BB′ spin system. The ^1J(Ag–P) coupling constants of 469 Hz (low field) and 498 (high field) are consistent with other ^1J(Ag–P) values measured in these 1:1 dimers, and the component of each doublet exhibits quartet additional fine structure thus indicating homonuclear ^2J(P–P) coupling to the

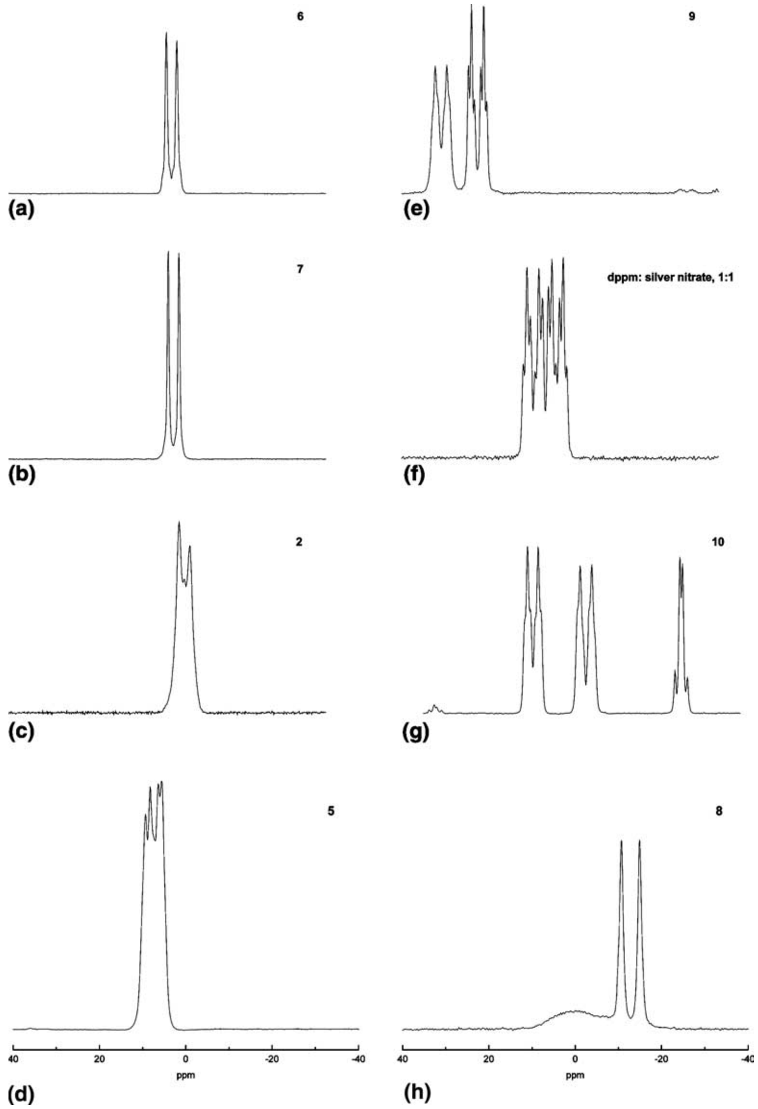

Fig. 5. Solid state 1D ^{31}P CPMAS of derivatives **6** (a), **7** (b), **2** (c), **5** (d), **9** (e), dppm:AgNO$_3$ 1:1 (f), **1** (g) and **8** (h).

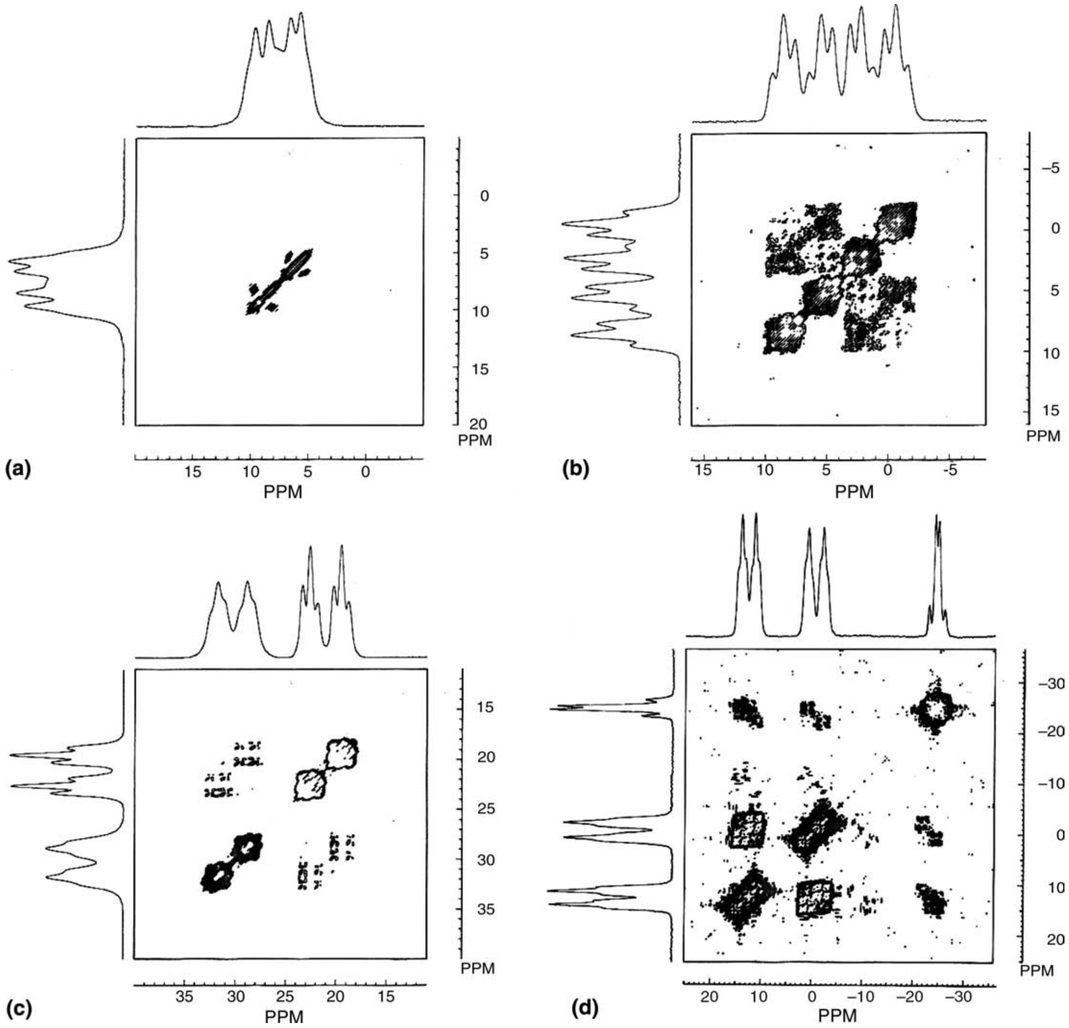

Fig. 6. Solid state 2D ^{31}P CPCOSY NMR spectra of derivatives **5** (a), **9** (b), dppm:AgNO$_3$ 1:1 (c) and **1** (d).

other P positions. This coupling is corroborated by the associated 2D ^{31}P CPCOSY spectrum of Fig. 6(b) which shows well-formed correlations above and below the main diagonal. A similar scenario is observed for the [AgNO$_3$(dppm)]$_2$ dimer [20] in Fig. 5(f). This example is more resolved in the 1D CPMAS spectrum, yielding ^1J(Ag–P) coupling constants of 498 Hz (low field) and 459 Hz (high field) which are comparable to those measured for the corresponding NO$_2$ dimers. However, the 2D ^{31}P CPCOSY result of Fig. 6(c) exhibits poorly formed, diffuse off-diagonal correlations that suggest an analogous AA′XX′BB′ spin system where less precise chemical shift overlap is being observed in comparison to the [AgNO$_2$(dcpm)]$_2$ (**9**) case. The 3:2 complex [(AgNO$_2$)$_2$(dppm)$_3$] (**1**) shown in Fig. 5(g) is a more complicated extension of this type of spin system, and probably warrants an AA′XX′BB′CC′ description. An earlier synthesis of the [(AgNO$_3$)$_2$(dppm)$_3$] analogue [2] demonstrated that the NO$_3$ anion was non-coordinating and that the trigonal planar, tri-bridged dimer generated near-chemical equivalence amongst all six P positions. In this NO$_2$ example no such chemical equivalence amongst the P sites is evident; from Fig. 5(g) it is readily observed that significant chemical shift differences exist between the three resolved ^{31}P resonances. This chemical shift range is >35 ppm, and the spectrum describes a system where a significant reduction in symmetry has been induced, probably by the direct coordination of NO$_2$ onto this tri-bridged dimer. The higher field resonance at −24.95 ppm is associated with the P positions that would be directly affected by such a coordination, while the other shifts at −0.81 ppm and 12.52 ppm are expected to be those positions with diphenyl substituents only. The P sites bearing diphenyl substituents yield ^1J(Ag–P) coupling constants of 439 Hz (low field) and 478 Hz (high field) which are consistent with the above mentioned measurements. However, the NO$_2$ influenced P position exhibits a reduced ^1J(Ag–P) value of ~ 370 Hz. The 2D ^{31}P CPCOSY spectrum of Fig. 6(d) displays correlations from each P site to all other P sites thus confirming this trigonal planar-type connectivity.

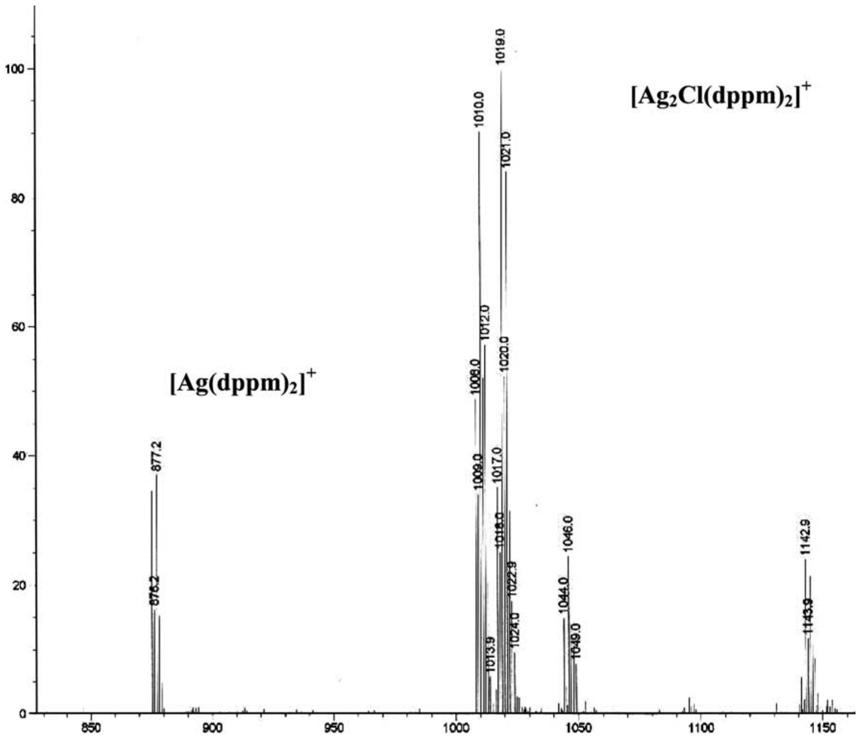

Fig. 7. ESI MS spectrum of derivative **2**.

The positive electrospray mass spectra of complexes **1**–**12** (the most relevant data are reported in Section 2 and a typical spectrum is reported in Fig. 7) indicate that these derivatives always undergo loss of the anionic NO_2^- ligand. The isotopic distribution of these species is in accord with the calculated composition. The aggregation behavior is strongly dependent on the stoichiometry of the adducts, but differs from that previously found for triorganophosphine adducts, in this case being independent of the solvent employed, no adducts containing CH_3CN being detected also at concentration 10^{-4} M, no significant differences being found between the spectra carried out in CH_3CN and those in acetone. Under our conditions in the case of dppm and dcpm ligands, aggregates containing two silver atoms, two diphosphine donors and one NO_2 group dominate significantly over adducts containing one, three or more silver atoms, whereas all other ligands seem to favor in solution aggregates containing only one silver center four-coordinated by two diphosphine donors In some cases oxidation of the phosphine is also evident. It is interesting to note that the behavior of dppet is unique, the most abundant ion being that containing two silver atoms, one NO_2 and three P_2-donors, as in the solid-state structure of $[Ag_2(dppm)_3]^{2+}$. No fragments containing two positive charges have been detected. As previously reported by us the negative electrospray spectra are always dominated by the presence of molecular peaks due to $[AgCl_2]^-$, $[Ag(NO_2)_2]^-$, $[Ag_2(NO_2)_3]^-$ [33].

3.3. X-ray discussion

The results of the low-temperature single crystal X-ray structure determinations are consistent with the formulation of the adducts formed between silver(I) nitrite and bidentate diphosphine ligands $Ph_2P(CH_2)_n$-PPh_2 ($n = 1$, 3) (**2**, **5**) and p-tolyl$_2P(C_{10}H_6)_2P$-p-tolyl$_2$ (**10**) as complexes of 1:1 stoichiometry, the former being centrosymmetric dimers with one $AgNO_2$:L formula unit comprising the asymmetric unit of the structure, the latter a mononuclear chiral species, two molecules of similar chirality comprising the asymmetric unit of the structure, the absolute configuration as determined being consistent with that expected for the ligand as supplied. The adduct (**8**) formed with $Ph_2PCH{:}CHPPh_2$ is tetranuclear, also centrosymmetric, of 2:1 $AgNO_2$:L stoichiometry, one such formula unit comprising the asymmetric unit of the structure. The crystal packings in a number of the arrays show features of interest.

The two crystallographically independent molecules of $AgNO_2$:p-tolyl$_2P(C_{10}H_6)_2P$$p$-tolyl$_2$ (1:1) (**10**) are closely similar (Fig. 8), with quasi-2 symmetry, the putative 2-axis passing through N, Ag and the mid-point of the binaphthyl central bond, the symmetry being broken principally by ill-behaved nitrite groups in both molecules. Interestingly, the principal difference between the two molecules occurs in respect of the inclinations of ring 2 at each phosphine; within each molecule, the pair conform to 2-symmetry, but are twisted (in concert?) in one molecule

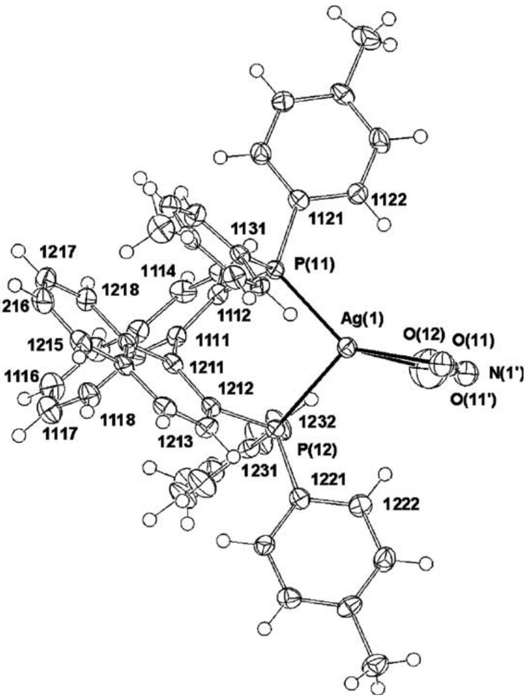

Fig. 8. Projection of molecule 1 of mononuclear $AgNO_2$:(*p*-tolyl$_2PC_{10}H_6C_{10}H_6$. P*p*-tolyl$_2$) (1:1) (**10**) normal to their AgP_2 planes.

relative to the other (Table 4). The environments of the silver atoms are bis(chelate) in each case, the chelates being one of small (NO_2) and one of large (L) bite. A recent report [27] has described the observation of similar $P_2Ag(O_2N)$ environments in the context of unidentate tertiary phosphine donors PR_3 for R = Ph, cy, *o*-tolyl (all 153 K studies); Ag–P are 2.4303(6), 2.4325(6); 2.459(1), 2.461(1); 2.4416(5), 2.4437(5) Å, with P–Ag–P 129.57(2), 132.03(5), 148.04(2)°, respectively. In the present context of a bidentate ligand P–Ag–P is constrained to a much smaller value than the above; despite this Ag–P are very similar. (The (not unusual) difficulties associated with the modelling of the nitrite group preclude meaningful comment on relevant geometries associated with it.) Ag–P–C(binap) are considerably smaller than Ag–P–C(Ph).

The two adducts $AgNO_2:Ph_2P(CH_2)_nPPh_2$ $(1:1)_2$ ($n = 1, 3$) (**2**, **5**) (Figs. 9 and 10) take a similar form; both are centrosymmetric dimers, in which the diphosphine ligand bridges the two silver atoms, a nitrite chelating each of the latter. In each case, the nitrite plane lies approximately normal to the line joining the mid-points of the two ligands, O(1) directed toward the centrosymmetrically related silver, albeit at a long distance, with the possibility in the $n = 3$ case that the O(1)$\cdots$O(1′) interaction is repulsive. Despite differences in P–Ag–P, the Ag–P distances are similar and similar to those discussed in the context of the unidentate mononuclear species above. The methylene bridge aside, ligand conformations (about the phosphorus atoms) are remarkably similar in the two complexes.

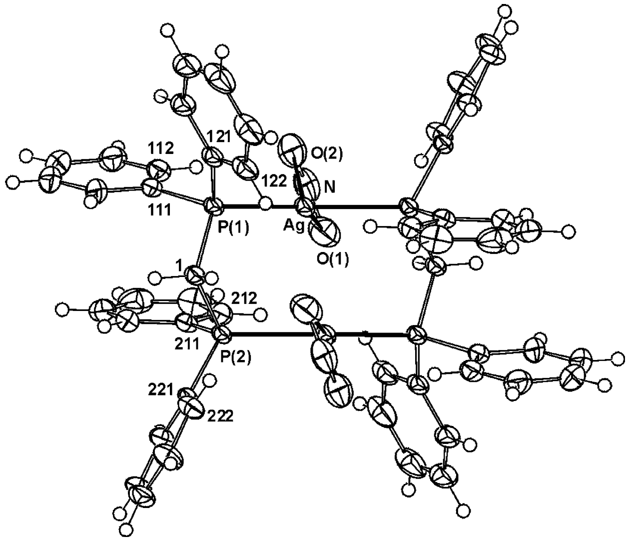

Fig. 9. Projection of the dimer $AgNO_2:(Ph_2PCH_2PPh_2)$ $(1:1)_2$ (**2**).

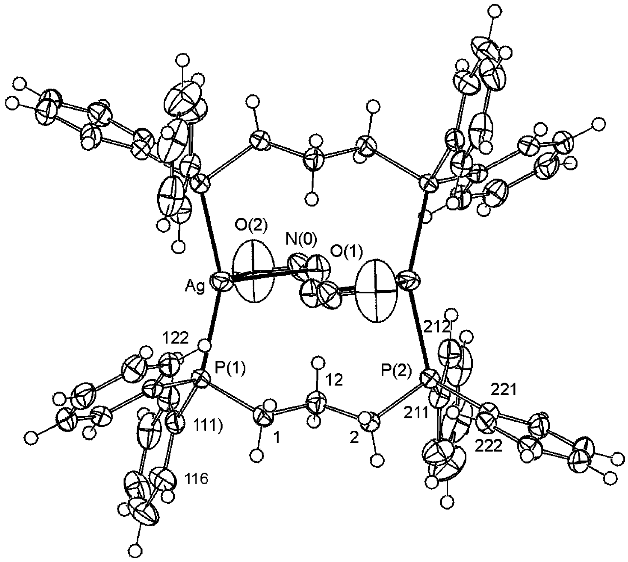

Fig. 10. Projection of the dimer $AgNO_2$: $Ph_2P(CH_2)_3$ PPh_2 $(1:1)_2$ (**5**).

Adducts of the form $MX:EPh_3$ (1:1) (MX = coinage metal(I) halide) are commonly tetrameric, occurring in the ‘cubane’ or ‘chair’ forms [34]. A recent study of $AgBrO_3:PPh_3$ (1:1) shows it also to be tetrameric, with a structure loosely based on the ‘chair’ tetramer, the central μ_3-halides being supplanted by μ_2-bridging oxygens from bromate oxyanions, with a second oxygen from each performing the third bridging function to a peripheral metal atom; the peripheral μ_2-halides are replaced by *O*·BrO·*O* anions, the two donor oxygens bonded to central and peripheral silver-atoms, respectively [35]. The present $AgNO_2:(Ph_2PCH{:}CHPPh_2)$ (2:1) adduct **8** (Fig. 9, Table 5) is a further variation on that theme, corresponding more nearly to having an origin in the $MX:Ph_2PCH_2PPh_2$ $(2:1)_2$ adducts which are also

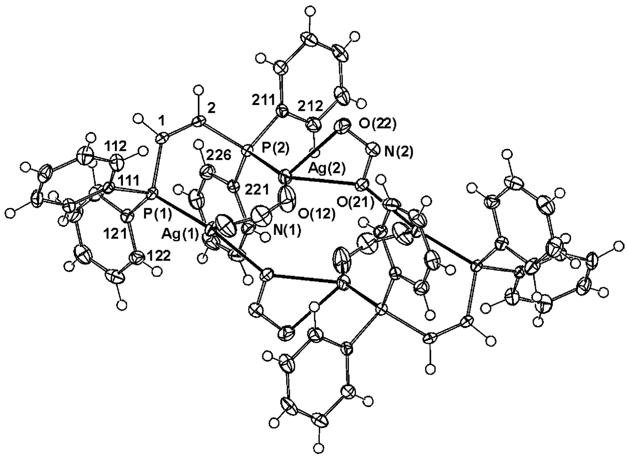

Fig. 11. Projection of tetranuclear $AgNO_2$: (Ph_2PCH:$CHPPh_2$) (2:1)$_2$ (**8**).

tetranuclear and of the chair form, the bidentate ligands bridging central and (alternate) peripheral metal atoms [36–39]. Here, however, the central 'plane' may be regarding as derivative of Ag(2) and O(21) and their centrosymmetric images, the O(22) filling a further coordination site on Ag(2), and O(21) bridging to peripheral Ag(1); the peripheral anion role bridging Ag(1) and the Ag(2) image is filled again by an *O*·X·*O* oxyanion, this time *O,O* (anion 1). The *cis*-bidentate phosphine in this complex, however, bridges the two silver atoms Ag(1,2) associated with the *same* Ag_2X_2 peripheral plane of the chair. Significant perturbations are found within the nitrite geometries, broadly correlating with the nature of the oxygen functionality.

4. Conclusion

This work demonstrates that it is possible to prepare and isolate diphosphine complexes of silver(I) nitrite of different nuclearity and stoichiometry. The dppm, dppe, dppp and dppb derivatives can persist in solution indefinitely, whereas the silver species containing chiral diphosphine ligands are generally more unstable. The stoichiometry and structure are strongly dependent on the nature of the phosphorus donors: dppm and dcpm, which generally act as bridging ligands, yielded dinuclear species, whereas the chelating dppe, S-Binap, R-TolBinap, S-diop and dppf yielded mononuclear pseudo-tetrahedral silver (I) species. With dppet a tetranuclear derivative of the chair form has been obtained, the bidentate ligands bridging central and peripheral silver centers whereas, likely, polymeric compounds have been obtained when a longer methylene chain $(CH_2)_4$ connects the two P atoms. However the synthesis of species of different nuclearity can be also ascribed to the peculiar features of the nitrite, which can be ionic as in the derivative $[Ag(dppe)_2]NO_2$, or bridiging tridentate as in $[(AgNO_2)_2(dppet)]_2$, or finally chelating as in $[(AgNO_2)_2(dppm)_2]$ and $[(AgNO_2)_2(dppp)_2]$, where the two Ag–O distances are sensibly different, and in $[AgNO_2(R)$-Tol-Binap)] where the two Ag–O distances are closer.

Acknowledgements

This work was supported by University of Camerino, MIUR and Carima Foundation.

References

[1] S.P. Neo, Z.-Y. Zhou, T.C.W. Mak, T.S.A. Hor, Inorg. Chem. 34 (1995) 520.
[2] D.M. Ho, R. Bau, Inorg. Chem. 22 (1983) 4073.
[3] E.R.T. Tiekink, Acta Crystallogr., C 46 (1990) 235.
[4] A.F.M.J. van der Ploeg, G. van Koten, A.L. Spek, Inorg. Chem. 18 (1979) 1052.
[5] A.F.M.J. van der Ploeg, G. van Koten, Inorg. Chim. Acta 51 (1981) 225.
[6] M. Sawamura, H. Hamashima, Y. Ito, J. Org. Chem. 55 (1990) 5935.
[7] S.J. Berners-Price, P.J. Sadler, Struct. Bonding (Berlin) 70 (1988) 27.
[8] A. Yanagisawa, Y. Nakatsuka, K. Asakawa, M. Wadamoto, J. Kageyama, H. Yamamoto, Bull. Chem. Soc. Jap. 74 (2001) 1477.
[9] M. Ohkouchi, M. Yamaguchi, T. Yamagishi, Enantiomer 5 (2000) 71.
[10] A. Yanagisawa, Y. Nakatsuka, K. Asakawa, J. Kageyama, H. Yamamoto, Synlett 1 (2001) 69.
[11] A. Yanagisawa, H. Nakashima, A. Ishiba, H. Yamamoto, J. Am. Chem. Soc. 118 (1996) 4723.
[12] S.P. Crabtree, A.S. Batsanov, J.A.K. Howard, M. Kilner, Polyhedron 17 (1998) 367.
[13] M.-C. Brandys, R.J. Puddephatt, J. Am. Chem. Soc. 124 (2002) 3946.
[14] G. Bodenhausen, R.L. Vold, R.R. Vold, J. Magn. Reson. 37 (1980) 93.
[15] D. Marion, K. Wuthrich, Biochem. Biophys. Res. Commun. 113 (1983) 967.
[16] T. Allman, J. Magn. Reson. 83 (1989) 637.
[17] J.V. Hanna, M.E. Smith, S.N. Stuart, P.C. Healy, J. Phys. Chem. 96 (1992) 7560.
[18] M.W. Senko, IsoPro Isotopic Abundance Simulator, vol. 2.1, National High Magnetic Field Laboratory, Los Alamos National Laboratory, Los Alamos, NM.
[19] S.R. Hall, D.J. du Boulay, R. Olthof-Hazekamp (Eds.), The XTAL 3.7 System, University of Western Australia, 2001.
[20] M. Hong, D. Wu, H. Liu, T.C.W. Mak, Z. Zhou, D. Wu, S. Li, Polyhedron 16 (1997) 1957.
[21] K. Nakamoto, J. Fujita, H. Murata, J. Am. Chem. Soc. 80 (1958) 4817.
[22] B.M. Gatehouse, J. Inorg. Nucl. Chem. 8 (1958) 79.
[23] K. Shobatake, C. Postmus, J.F. Ferraro, K. Nakamoto, Appl. Spectrosc. 23 (1969) 12.
[24] D. Perreault, M. Drouin, A. Michel, V.M. Miskowski, W.P. Schaefer, P.D. Harvey, Inorg. Chem. 31 (1992) 695.
[25] A. Cingolani, Effendy, F. Marchetti, C. Pettinari, B.W. Skelton, A.H. White, J. Chem. Soc., Dalton. Trans. (1999) 4047.

[26] M.A. Hitchman, G.L. Rowbottom, Coord. Chem. Rev. 42 (1982) 55.

[27] R.T. Stibrany, J.A. Potenza, H.J. Schugar, Inorg. Chim. Acta 243 (1996) 33.

[28] R.J. Goodfellow, Post-transition metals, copper to mercury, in: J. Mason (Ed.), Multinuclear NMR, Plenum Press, New York, 1987, pp. 563–589 (Chapter 21).

[29] E.L. Muetterties, C.W. Alegranti, J. Am. Chem. Soc. 94 (1972) 6386.

[30] R.G. Goel, P. Pilon, Inorg. Chem. 17 (1978) 2876.

[31] M. Ohkouchi, D. Masui, M. Yamaguchji, T. Yamagishi, J. Mol. Catal. A 170 (2001) 1.

[32] Z. Yuan, N.H. Dryden, J.J. Vittal, R.J. Puddephatt, Can. J. Chem. 72 (1994) 1605.

[33] A. Cingolani, Effendy, M. Pellei, C. Pettinari, C. Santini, B.W. Skelton, A.H. White, Inorg. Chem. 41 (2002) 6633.

[34] G.A. Bowmaker, Effendy, R.D. Hart, J.D. Kildea, A.H. White, Aust. J. Chem. 50 (1997) 653.

[35] A. Cingolani, Effendy, J. Hanna, M. Pellei, C. Pettinari, C. Santini, B.W. Skelton, A.H. White, Inorg. Chem. 42 (2003) 4938.

[36] G. Nardin, L. Randaccio, Cryst. Struct. Commun. 3 (1974) 607.

[37] A. Camus, G. Nardin, L. Randaccio, Inorg. Chim. Acta 12 (1975) 23.

[38] S. Ramaprabhu, N. Amstutz, E.A.C. Lucken, G. Bernardinelli, J. Chem. Soc., Dalton Trans. (1993) 871.

[39] P.A. Pérez-Lourido, J.A. Garciá-Vázquez, J. Romero, M.S. Louro, A. Sousa, Q. Chen, Y. Chang, J.A. Zubieta, J. Chem. Soc., Dalton Trans. (1996) 2047.